Reducing Pixel Artifacts Around Point Sources in C-BASS Maximum Likelihood Maps.

Isabel Leatherman, supervised by Prof Jonathan Sievers

This manuscript was compiled on December 11, 2019

The C-BASS all sky survey maps the polarization and intensity of the sky in the 5GHz frequency range in order to make accurate foreground maps for subtraction from CMB data. However, the model of the measured data in maximum likelihood mapping does not accurately describe the pixelized data. The pixelization errors introduced by this model error then result in significant artifacts around point sources. The XGLS estimate attempts to account for these errors by adding an extra term in the noise covariance matrix, however solving this is very computationally expensive. In this report I outline a faster method, in which the pixelization error is instead solved for as part of the maximum likelihood solution, and detail the calculation of the added part of the solution and its implementation on the C-BASS data. The maps generated using this method are shown and the initial success in reduction of artifacts is discussed.

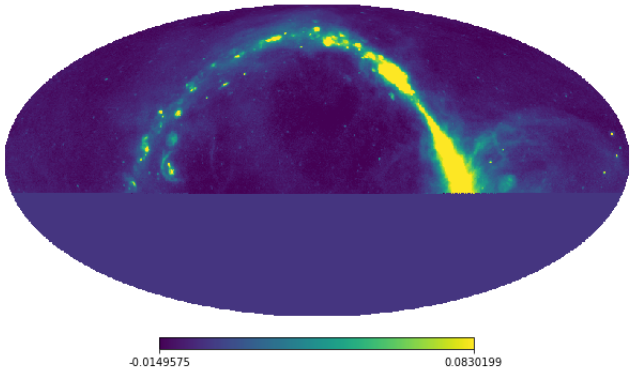

Fig. 1. The map of the C-BASS northern telescope data using the maximum likelihood mapping. Only the northern telescope data is mapped, which leads to the cutoff in the lower third of the map.

1. Introduction

The cosmic microwave background (CMB) radiation is a massive source of cosmological information, and as such there is a lot of work being done to survey and map the whole sky. However, there is the danger that foreground emission could be mistaken for CMB radiation, and therefore we need to be able to model foreground emission with high accuracy in order to be able to subtract the foreground from CMB observations. The C-Band All-Sky Survey (C-BASS) project aims to map the intensity and polarization of the whole sky at 5Ghz, a frequency at which synchotron, free-free, and anomalous microwave emission dominate, and CMB emissions are subdominant(1). C-BASS consists of two telescopes. The northern telescope, located at the Owens Valley Radio Observatory in California finished its survey in 2015, and the southern telescope, located in the Karoo Desert in South Africa, is still collecting data.

The C-BASS data, and similarly sampled data, can be mapped using a maximum likelihood estimator. However, the sky is continuous and our mapping is not, and so the predicted model will not accurately describe the actual data. The local pixelization errors introduced by this model error are then propagated into neighbouring pixels by the noise correlation. This in turn leads to significant artifacts around point sources, where the pixel gradient is very high. Previous solutions required prior knowledge about the location and amplitude of these point sources, for example subtracting the point sources from the data entirely(2). A solution that doesn't require this previous knowledge is to add an extra term in the data model to account for the pixelization error. A previous implementation of this idea is the Pixel Noise estimate (XGLS) (3), however this estimate has a very high computational cost.

In this report I outline an alternative faster solution of accounting for the pixelization error which relies on computing the gradient of the data from a prior solved map of the same sampled data. I will detail my implementation of this solution on the northern C-BASS data using the python library `minkasi`*, and discuss its effects on the artifacts surrounding point sources.

In section 2, I go over the Maximum Likelihood mapping method that gives rise to these artifacts. In section 3 I explain the XGLS estimate and its cost. In section 4 I detail the different approach that I implement in the mapping, and the calculation of the data gradient is described in section 5. I discuss the resulting maps in section 6, and summarize my conclusions in section 7.

2. Maximum Likelihood Mapping

The time sampled data measured by C-BASS is usually modeled by

$$d = Am + n. \quad [1]$$

Here, d is the vector of the raw time-ordered data (TOD) samples measured by the telescope. A is the matrix that holds the information of within which pixel each sample is located on the sky, called the pointing matrix. The vector n is the noise of each sample, with covariance matrix N. The vector m is the vector of pixels in the sky image, where each m_i is the value held in pixel i. The maximum likelihood map is then found by minimizing the χ^2 of the model:

$$\chi^2 = (d - Am)^T N^{-1} (d - Am) \quad [2]$$

This leads to a maximum likelihood solution

$$m = (A^T N^{-1} A)^{-1} A^T N^{-1} d. \quad [3]$$

*https://github.com/sievers/minkasi

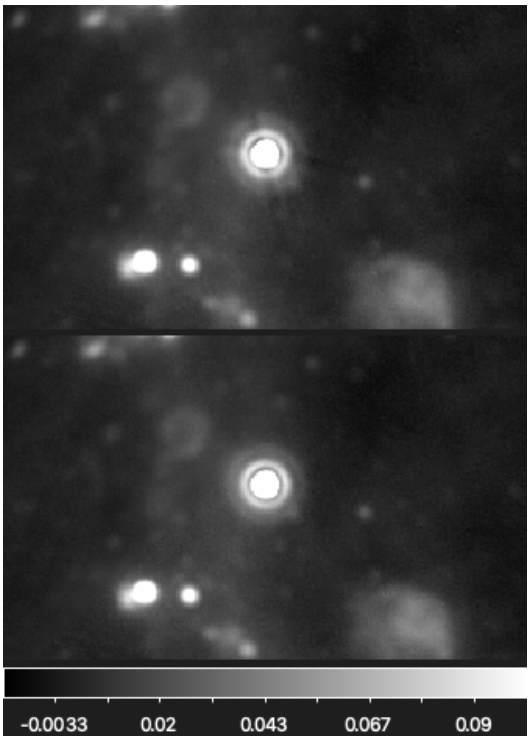

Fig. 2. Top: A point source in the maximum likelihood mapping for the C-BASS northern telescope data, where the artifacts around the point source are clearly visible. Bottom: The same point source but from the new pipeline, where the artifacts have been significantly reduced.

However, $A^T N^{-1} A$ is often not invertible, so we can equivalently solve

$$(A^T N^{-1} A)m = A^T N^{-1} d. \quad [4]$$

instead. In the `minkasi` pipeline, the iterative preconditioned conjugate gradient (PCG) is used to solve equation 4. A map made using this estimation can be seen in figure 1.

The artifacts in the maps generated using this estimate arise because equation 1 does not accurately predict the pixelized data. The maximum likelihood estimation is particularly problematic when predicting the pixel data near areas with large gradients, such as bright point sources. As the noise n is the only term in equation 1 that can account for these errors, the correlation of N spreads this error out to surrounding pixels in a way that is difficult to predict. For C-BASS data, they manifest in an X around the point source, as seen in figure 2.

3. The XGLS Estimate

The XGLS estimate accounts for the pixelization errors by adding a term to the data model, eq. 1.

$$d = Am + n + x \quad [5]$$

Here, the extra term x is treated as part of the total noise. This is then reflected by an extra term in the noise covariance matrix, $N_{tot} = N + X$, where X is the covariance matrix of x. Similarly to the maximum likelihood estimate, this leads to the solution

$$m = (A^T (N + X)^{-1} A)^{-1} A^T (N + X)^{-1} d. \quad [6]$$

. However, the inverse of N_{tot} is also very hard, if not impossible, to compute. Here PCG can again be used to solve the system $(N + X)w = v$ instead, but this then requires an entire run of the iterative PCG to solve this system for each iteration of the PCG used to solve equation 6(3). This exponentially increases the computational cost, which depending on the size of the dataset being mapped, can be dozens, if not hundreds, of times slower than the original maximum likelihood. Thus there is significant motivation to finding a more efficient way to deal with the pixelization errors.

4. Alternative Approach

The approach used in the `minkasi` pipeline is similar to the XGLS estimate in that it also models the data using equation 5. But the key difference is that we treat x as a part of the solution itself, rather than another noise term. To do this, an extra term must also be added to the χ^2.

$$\chi^2 = (d - Am)^T N^{-1} (d - Am) + x^T X^{-1} x \quad [7]$$

This is mathematically equivalent to the XGLS solution as they both lead to identical χ^2 minimums and maximum likelihood surfaces.

We can then rewrite equation 7 to focus on solely the high gradient pixels.

$$\chi^2 = (d - Am)^T N^{-1} (d - Am) + (p - m)^T Q^{-1} (p - m) \quad [8]$$

Here, Q is a diagonal matrix of the inverse variance of each pixel, and p is the vector of prior parameters. This is then minimized to obtain the maximum likelihood solution.

$$\frac{\delta \chi^2}{\delta m} = 0 = (A^T N^{-1} A + Q^{-1})m - A^T N^{-1} d - Q^{-1} p$$

$$(A^T N^{-1} A + Q^{-1})m = A^T N^{-1} d + Q^{-1} p \quad [9]$$

Because Q is a diagonal matrix, Q^{-1} is very easy to compute, and therefore only one PCG is needed to solve equation 9.

5. Calculating Q From the Pixel Gradient

Q is computed from the gradient of map of the data solved using the maximum likelihood estimation. In Python, the map itself is stored as a one dimensional array following the HEALPix partition of a sphere. Although functions exist to compute the gradient across this one dimensional array, the map itself is inherently both two-dimensional and spherical, and so gradient calculations must take that into account.

A. The HEALPix Structure. The Hierarchical Equal Area iso-Latitude Pixelization structure (HEALPix) divides the spherical sky into 12 equal area base-resolution pixels that sit in three rings around the poles and equator, as seen in figure 4.(4) The parameter N_{side} parameterizes the resolution of the projected map by defining the number of pixels along one side of a base-resolution pixel. This leads to a sphere divided into $4 \times N_{side} - 1$ isolatitude rings, with $4 \times N_{side}$ pixels along the equatorial ring. For C-BASS data, the resulting map has an N_{side} of 512. There are two pixel numbering schemes that turn these pixels into the 1D arrays. The one that is used with the C-BASS data is ring ordering, where the pixels are numbered around each latitude ring from the north to south pole.

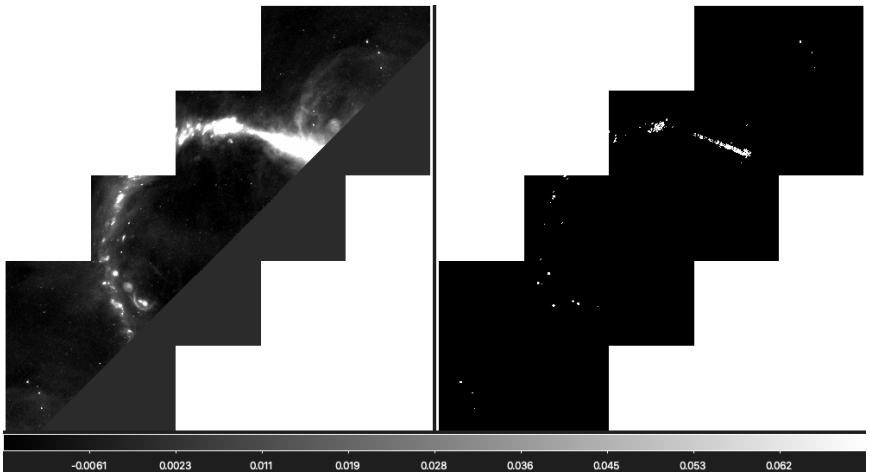

Fig. 3. Left: map of the data using the maximum likelihood mapping. Right: the zeroed gradient map of the same map, showing only the pixels with the steepest gradient. These gradients were then used to build the matrix Q in the alternative map, equation 4.

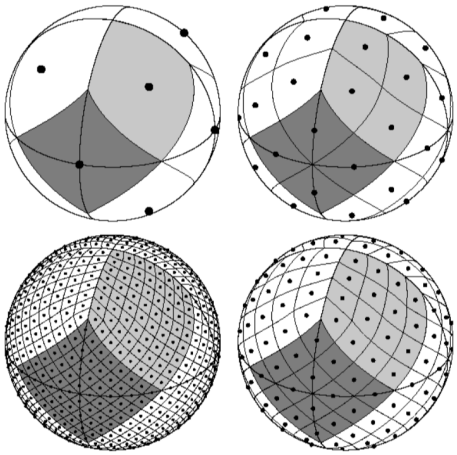

Fig. 4. The HEALPix pixelization of the sphere, from the HEALPix Primer (4). The top left is the base-resolution, the top right has $N_{side} = 2$, the bottom left has $N_{side} = 8$, and the bottom right has $N_{side} = 4$.

The HEALPix structure allows the discretization of functions along the surface of the sphere. In particular, it allows for the map to be converted to spherical harmonic representation. Spherical harmonics are a complete set of orthogonal functions on the sphere that can be used to represent any function, such as the map, that is also defined on the sphere. As the spherical harmonic representations are in spherical coordinates, I can then get the gradient in both the θ and ϕ directions for each pixel in the map. I then converted his gradient vector from radians to pixels by using the number of pixel rings in the θ direction, and the amount of pixels along the equator in the ϕ direction.

B. Zeroing the Pixel Gradient. As the majority of the map pixels are not part of a point source, the gradients across pixels are on average very low. Thus all gradients within three standard deviations from the mean were zeroed, leaving only the steepest 0.3% of the gradients. The resulting mask of a prior map can be seen in figure 3. This isolates both the numerous point sources across the map and the noisier signal across the galactic plane.

Q is then filled by

$$Q_{i,j} = \begin{cases} \frac{1}{grad_i^2} & \text{if } i = j \ \& \ grad \neq 0 \\ 0 & \text{otherwise} \end{cases}$$

where i is the index of the pixel, and $grad_i$ is the length of the gradient vector at the pixel i. The zeroing of the gradient can also be represented mathematically, with a mean gradient of μ and a standard deviation σ.

$$grad_i = \begin{cases} 0 & \text{if } \mu - 3\sigma \leq grad_i \leq \mu + 3\sigma \\ grad_i & \text{otherwise} \end{cases}$$

6. Results

Upon implementation of the `minkasi` pipeline on the C-BASS northern telescope data, with the Q calculated from the prior map, the resulting new maps display significant reduction in artifacts. This reduction for one specific point source can be seen in figure 2. In order to more clearly see the differences between the two maps, I also mapped the value difference between them. This results in a clearer image of the actual artifact reduction. An example of this can be seen in figure 5. It also reveals many more point sources with artifacts that aren't as obvious from the initial maximum likelihood mapping, seen in figure 6. A third result from the difference maps is the ability to also lend some more clarity to the more dense parts of the maps, such as the higher intensity of the galactic plane. Figure 7 is an example of this.

Another important result to note is the time that running this pipeline. This implementation was run using the data from the full survey of the northern C-BASS telescope, which is about 5,000 sets of time-oriented data. While running parallel on 20 processes, the original maximum likelihood estimation took about minutes on average. Conversely, the new estimation took about 54.5 minutes on average. While it should be noted that a prior map from the original maximum likelihood map is required for the alternative approach, this shows that these two methods have comparable computational cost. Thus it is very feasible that this new approach can be scaled upwards to larger sets of data.

A. Next Steps. While the initial results showing the significant reduction in artifacts are very promising, there are further

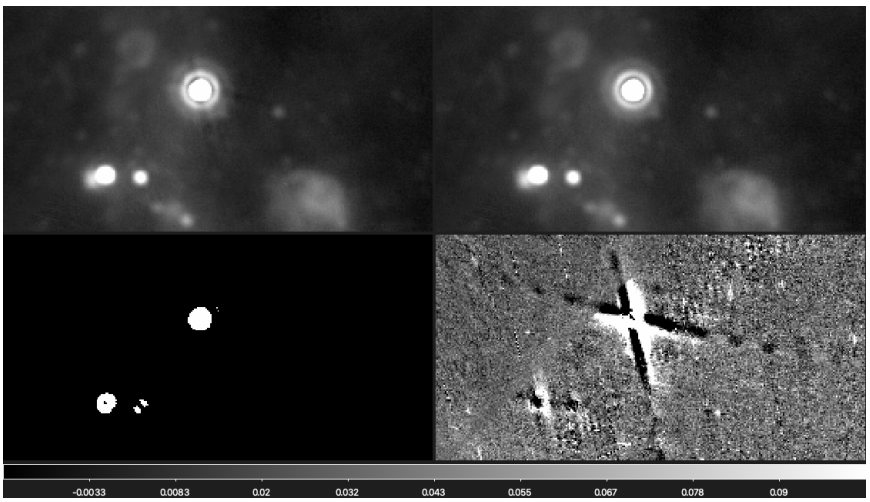

Fig. 5. Top left: A point source on the map of the data using the maximum likelihood mapping. Top right: The same point source but on the resulting map of the data. Bottom left: the zeroed gradient map of the maximum likelihood mapping at the same point source. Bottom right: The difference map between the two maps, clearly showing the reduction of the X artifact around the point source.

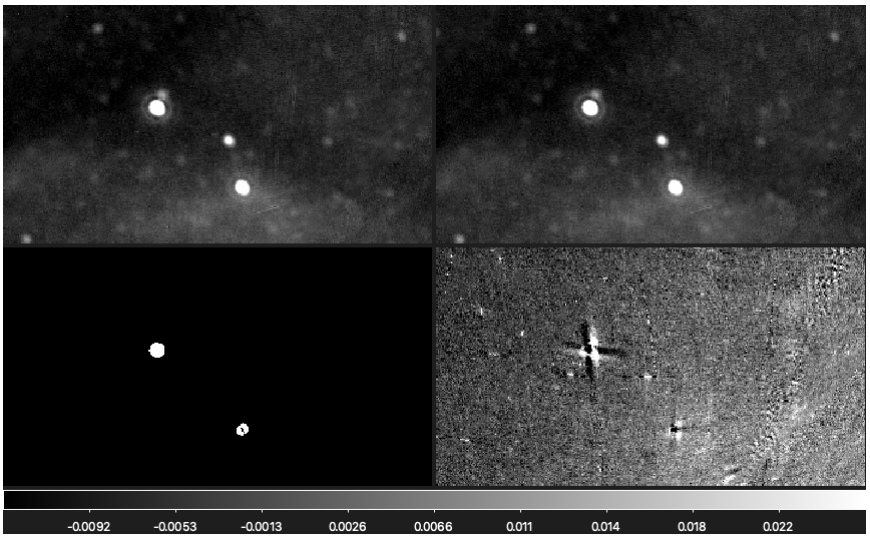

Fig. 6. Top left: A point source on the map of the data using the maximum likelihood mapping, where there is no immediately visible artifact. Top right: The same point source but on the resulting map of the data. Bottom left: the zeroed gradient map of the maximum likelihood mapping at the same point source. Bottom right: The difference map between the two maps, clearly showing an artifact around the point source.

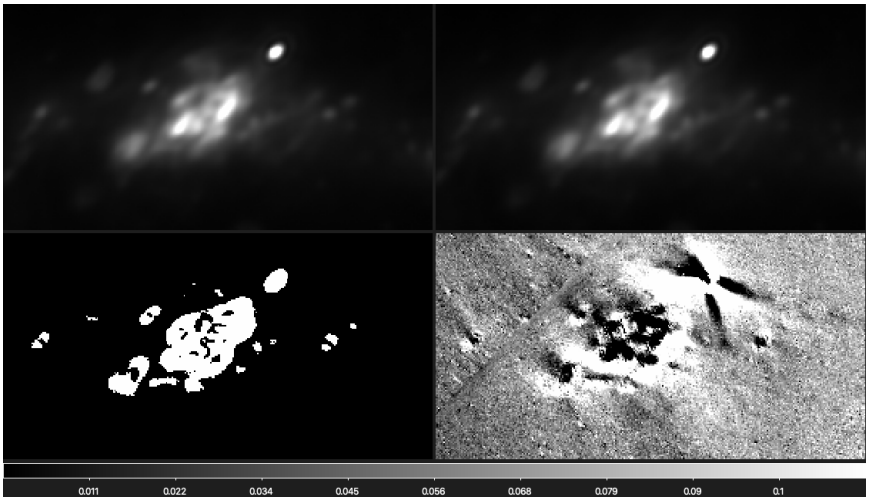

Fig. 7. Top left: A denser part of the galactic plane, scaled so that it is easier to see the structure. Top right: The same area but on the resulting map of the data. Bottom left: the zeroed gradient map of the maximum likelihood mapping at the same spot. Bottom right: The difference map between the two maps, revealing a much more complex change.

steps that can be taken in order to confirm the validity of the mapping. The `minkasi` pipeline supports the conversion of maps into the time domain of the TODs, and so it is possible to subtract both the maximum likelihood map and the new map from the data signal to get the residuals of each sample. The residuals from the maximum likelihood map should show a peak near point sources, whereas the residuals from the new map should show a much smoother plot.

Another important extension would be to ensure that the new mapping doesn't distort the power spectrum. By running multiple simulations with very finely sampled input data, the recovered power spectrum could then be compared to the power spectrum of the input data.

There could also be further analysis into the choice for the gradient cutoff. A less sparse matrix Q could lead to longer computation times, but there may be more previously unseen artifacts that can be reduced. The exact effects of such a change is a source for further investigation.

7. Conclusions

I outlined the use of a new maximum likelihood mapping to account for extra errors near point sources and the steps required to implement this, as well as its computational cost benefits over the XGLS estimate. The pipeline has some initial successful reductions of artifacts. With some more investigations to further confirm these results, the use of this new mapping pipeline would become very promising in making faster and more accurate foreground maps. As this is much faster than the XGLS estimate, it has even further application to data analysis. The reduced computational cost makes this a much more viable method to make accurate maps with telescopes producing much more data than C-BASS.

1. ME Jones, et al., The c-band all-sky survey (c-bass): design and capabilities. *Mon. Notices Royal Astron. Soc.* **480**, 3224–3242 (2018).
2. R Dünner, et al., The atacama cosmology telescope: Data characterization and mapmaking. *The Astrophys. J.* **762**, 10 (2012).
3. L Piazzo, Least squares image estimation for large data in the presence of noise and irregular sampling. *IEEE Transactions on Image Process.* **26**, 5232–5243 (2017).
4. KM Gorski, BD Wandelt, FK Hansen, E Hivon, AJ Banday, The healpix primer. *arXiv preprint astro-ph/9905275* (1999).